FASTC-ID(RS)T-0826-92

FOREIGN AEROSPACE SCIENCE AND TECHNOLOGY CENTER

COMPUTATIONAL METHOD IN OPTIMAL BENDING-TWISTING COMPREHENSIVE DESIGN OF WINGS OF SUBSONIC AND SUPERSONIC AIRCRAFT

by

Liu Dehua, Huang Changyou, et al.

HUMAN TRANSLATION

FASTC-ID(RS)T-0826-92 25 February 1993

MICROFICHE NR:

COMPUTATIONAL METHOD IN OPTIMAL BENDING-TWISTING COMPREHENSIVE DESIGN OF WINGS OF SUBSONIC AND SUPERSONIC AIRCRAFT

By: Liu Dehua, Huang Changyou, et al.

English pages: 15

Source: Kongqidonglixue Xuebao, Vol. 7, Nr. 2,
June 1989; pp. 192-198

Country of origin: China
Translated by: Leo Kanner Associates
F33657-88-D-2188
Requester: FASTC/TATV/Paul F. Freisthler
Approves for public release; Distribution unlimited.

GRAPHICS DISCLAIMER

All figures, graphics, tables, equations, etc. merged into this translation were extracted from the best quality copy available.

COMPUTATIONAL METHOD IN OPTIMAL BENDING-TWISTING COMPREHENSIVE DESIGN OF WINGS OF SUBSONIC AND SUPERSONIC AIRCRAFT

Liu Dehua, Huang Changyou and Zhu Guolin of China Aerodynamics Research and Development Center; and Li Yupu and Xie Guangming of Institute No. 611, Ministry of Aeronautics and Astronautics Industry

Abstract

The paper presents a computational method in the optimal bending-twisting comprehensive design of wings of subsonic and supersonic aircraft; a method for obtaining the finite fundamental solution is applied. By selecting a design point (M number and C_L) at each of subsonic and supersonic aircraft, the designing of wings to withstand bending and twisting is carried out. The goal is to reduce lift-related drag. On this technical basis, the aerodynamic features of these two design points of subsonic and supersonic aircraft are noted in addition to the feasibility of other aircraft performance values applied to its structure. The paper presents the computational results of the optimal bending-twisting design for subsonic aircraft, the optimal bending-twisting design of supersonic aircraft, as well as the comprehensive design. As analysis showed, the computational results are rational.

Key terms: subsonic air flow, supersonic air flow, bending-twisting, and design of aircraft wings.

I. Introduction

In the design and model selection stage, to achieve lower drag, the bending-twisting design of aircraft wings should be carried out in the aircraft design department; this necessity thus urgently dictates that a computational method be devised for the optimal bending-twisting comprehensive design for wings of subsonic and supersonic aircraft.

The paper presents a method for comprehensive design. This method is based on the principle that air flow obeys a linearized weak perturbation equation. At supersonic aircraft speeds, the finite fundamental solution method is used to derive a matrix equation relating drag and air pressure difference. Based on the restrained lift and force moments, the Lagrangian multiplier is employed to derive the drag function. Based on the functional principle of deriving extreme values, linear algebraic equations for minimum drag are established. By solving this set of equations, the optimal bending surface shape of aircraft wings can be obtained.

By utilizing the horseshoe-shaped eddy mesh method for subsonic aircraft and based on the given chordwise pressure distribution, the drag function is derived given the constraints of dip and elevating force moment, and the lift coefficient in design is used to arrive at the coefficient of proportionality of the chordwise load distribution for minimum drag, thus advancing a further step to determine the shape of optimal bending surface for the aircraft wings.

For a given shape of aircraft wing surface, after carrying out the optimal bending-twisting design with the selected design points for subsonic and supersonic aircraft, frequently in actually designing aircraft wings based on computations, the wing camber and twist angle of wing are too large, thus making it difficult to apply the outcome to the aircraft structure and thus bringing about lack of coordination with other aircraft performance values; in addition, it is difficult to apply simultaneously the design points of subsonic and supersonic aircraft. Hence, a comprehensive design method is required. For example, by appropriately combining bending and twisting when designing subsonic and supersonic aircraft in order to make allowance for various aircraft performance aspects, this will also make aircraft drag as small as possible in order to achieve a practicable computer program that is adaptable to first-stage aircraft wing design.

A comprehensive computer program of bending-twisting design of aircraft wing--front wing (and empennage) must exhibit the following functions: applicability to a single wing, to a canard wing--aircraft wing, and to an aircraft wing--empennage with possibly the upper swept-forward angle; and applicability to configurations of tandem wing, aircraft wing--wing tip winglet.

II. General Description of Method

The linearization theory of weak perturbation in aerodynamic design and computation, as well as the eddy lattice method of the finite fundamental solution are applied. Under the restraint of given coefficients of lift and moment of force, the wing-induced drag or lift-induced drag is minimized with introduction of the Lagrangian multiplier, applying the functional principle of deriving extreme value.

The paper will briefly explain the method. Refer to Reference [5] for details, bending-twisting design for minimum induced drag for subsonic aircraft, and the aerodynamic computation. See Reference [3, 4] for those related to supersonic aircraft. See Reference [5] for the principle and method of comprehensive design.

As the fundamental approach for the bending-twisting design of subsonic aircraft wing, the eddy mesh method is applied to the designing of the average-camber surface on surface of two lifts. This approach avoids the difficulty of specifying the chordwise load distribution in advance of aircraft wing design. For the configuration of two wing surfaces, the resultant solution of local surface inclination can satisfy two following conditions: minimum eddy drag given the design lift coefficient, and satisfying the condition that the dip and elevating force moment (around the origin) is zero. By applying the Lagrangian multiplier method, the spline extrapolation value method, and numerical integration, the bending-twisting shape of aircraft wing for minimum eddy drag under the designed lift coefficient can be obtained.

Between the local surface inclination and amount of circulation, there is the following relationship based on [2]:

$$\left\{\frac{\partial \bar{z}}{\partial \bar{x}}\right\} = [A] \left\{\frac{\Gamma}{U}\right\} \qquad (1)$$

In the equation, [A] is the matrix of aerodynamic effect coefficient.

By using the method recommended in [2], the circulation amount distribution and the span-direction coefficient of proportionality can be determined, thus determining the circulation amount matrix $\left\{\frac{\Gamma}{U}\right\}$, lift coefficient C_L, coefficient C_m of force moment, and coefficient C_{DV} of drag. At a point $(\xi', \bar{y})$ of the calculated plane, the equation of local camber is

$$\frac{\bar{z}'(\xi, \bar{y})}{c} = \int_{1}^{\xi'} \frac{\partial \bar{z}}{\partial \bar{x}} (\xi, \bar{y}) d\xi \qquad (2)$$

In this program, the local surface inclination among inclination points of the triple spline extrapolation value is used; also employed is the camber distribution of wing surface obtained from integrating the triple spline.

The fundamental concept and method of subsonic aerodynamic computation are similar to those of bending-twisting design. The fundamental computational equation can be rewritten from Eq. (1):

$$\left\{\frac{\Gamma}{U}\right\} = [A]^{-1}\left\{\frac{\partial \bar{z}}{\partial \bar{x}}\right\} \tag{3}$$

In the equation, $\partial \bar{z}/\partial \bar{x}$ is the inclination of wing surface mesh point; [A] is the aerodynamic effect coefficient matrix, which can be obtained from the similar method in bending-twisting design.

From Eq. (3), after solving for the circulation amount $\{\Gamma/U\}$ of various lattice-net points on the wing surface, lift of the aircraft wing, coefficient of force moment, and the induced drag can be computed from conventional aerodynamic formulas.

In the fundamental concept of bending-twisting design and computation of supersonic aircraft wing, a limited number of parallelogram meshes can be divided from the mid-arc surface of aircraft wing. Every parallelogram mesh can be considered as iterative addition of four semifinite triangular zones. A surface eddy with constant u is placed in each semifinite triangular zone. See [3, 4] for details of computational formula for induced velocity generated at a control point of the above-mentioned surface eddy.

After placing a surface eddy with constant u on the mid-arc surface of the aircraft wing, the algebraic equation satisfying normal direction non-penetration at the wing surface is

$$[A]\{P\} = \left\{\frac{d\bar{z}}{d\bar{x}} - \alpha\right\} \tag{4}$$

In the equation, [A] is matrix of the aerodynamic effect coefficient; $\{d\bar{z}/d\bar{x}\}$ is the inclination at various control points on the wing surface; $\{P\}$ is the intensity of the wing surface eddy; and a is the incident angle of incoming flow.

By using the constraint of lift and force moment, the drag function is derived. By applying the conditions on deriving extreme value with computation and manipulation, a set of equations as follows can be obtained.

$$\sum_{i=1}^{N_w}(A_i a_{ij} + A_j a_{ji})P_i + \lambda_1(-A_i) + \lambda_2 A_i(x_i - \bar{x}) = 0 \tag{5}$$

$$\sum_{i=1}^{N_w} A_i P_i + \bar{L} = 0 \tag{6}$$

$$\sum_{i=1}^{N_w} A_i P_i (x_i - \bar{x}) - \bar{M} = 0 \tag{7}$$

See [3, 4] for derivation details. In the equations, A_i is the area of the mesh; $\bar{x}$ is the x coordinate of the center of the force moment; $\bar{L}$ is the constraint lift; $\bar{M}$ is the condition of force moment; a_{ij} is the effect coefficient; and N_w is the number of blocks into which the aircraft wing has been divided.

By solving Eqs. (5), (6) and (7), we can obtain the eddy intensity P_i on the aircraft wing; the inclination at various control points on the mid-arc surface can be obtained.

$$\left(\frac{dz}{dx}\right)_i = \alpha + \sum_{i=1}^{N_w} a_{ij} P_j \tag{8}$$

Thus, the shape of the mid-arc surface of aircraft wing can be determined.

The fundamental philosophy in the bending-twisting comprehensive design of aircraft wing--canard wing (or empennage) can be summarized into four following points:

1. Determine the site of the datum station in bending-twisting comprehensive design

In this paper, the locations of three stations at half-span length are selected. Their spanwise locations are wing tip, half-span length about 50 percent, and exposed wing root. The bending-twisting data at the locations of other spanwise stations can be obtained from data linearized extrapolation values.

2. Arrangement of twisting degree (angle) and tradeoff of camber

In the comprehensive design, first the bent-twisted exterior of the wing surface obtained from the design is dissolved into twisting degree (twisting angle) and camber.

To make allowance for other aircraft performance aspects, the arrangement method of twist angle data input is adopted for the twist angle at various spanwise stations of the aircraft wing. In the program, compile the arrangement scheme of the twist angle for 10 different sets capable of being inputted for the purpose of computational comparison and selection.

As for the camber tradeoff, the aircraft wing camber data $\bar{f}_{.}$ and $\bar{f}$ (obtained from subsonic and supersonic aircraft design) are subjected to a tradeoff according to certain rules.

$$\bar{f}_{.} = K_{.}\bar{f}_{.} + K_{.}\bar{f}_{.} \qquad (9)$$

In the equation, $K_{.}$ and $K_{.}$ are the tradeoff ratios. During the initial tradeoff design, we can select $K_{.} = K_{.} = 0.5$. According to requirements, the values of $K_{.}$ and $K_{.}$ can be changed.

3. Arrangement of flaps at leading and trailing edges

In order to moderate the increment of induced drag or lift-induced drag for aircraft wing after conducting a tradeoff design, and to simultaneously heed two design points of subsonic and supersonic aircraft, a variable-camber technique for the aircraft wing was adopted. As indicated in the technique, the flaps of the leading and training edges are adopted. In design computations, there can be 1 to 3 blocks for the flaps at the leading and trailing edges; one inflexion point may exist at the leading edge of the flap; three sets of chordwise values for the flap can be selected; and the maximum flap camber assemblies can be as many as 5. In this design computation, a set of flap exterior and camber can be selected with minimum drag.

4. Wing pattern data for location of datum station

After inputting the distribution data of wing pattern thickness, finally the wing pattern data at the spanwise location of the datum station of the aircraft wing can be obtained.

III. Computational Results

Designing the camber surface of canard wing--aircraft wing proceeds with the exterior shape in first-stage aircraft design. Compute the relative positions of changing two wing surfaces at states of $M_\infty=0.85$, $C_{L.D}=0.2$, $a_c=0.3$, and $a_w=0.3$. Change the relative locations of two wing surfaces: $\bar{z}=-0.5$, -0.7, -0.84, -1.0, and -1.2; a total 5 positions. There are 6 states for the center of the force moment: moving forward for 10 and 5 percent, moving backward for 5, 10 and 15 percent, as well as the prototype for a total of 6 states. More than 30 sets of data were computed.

Fig. 1 indicates the canard wing layout. When $M_\infty=0.85$, $C_{L.D}=0.2$, $a_c=a_w=0.3$, and $\bar{z}_c/(b/2)=-0.172$, Fig. 1 shows the variation curve of the induced drag C_{DV} in the range of distributed flat points of the force moment.

Fig. 2 indicates the configuration of aircraft wing--canard wing. The figure indicates the distribution of twist angles for different vertical separate positions of aircraft wings and canard wings for the case of $M_\infty=0.85$, $C_{L.D}=0.2$, $a_c=a_w=0.3$, and $\bar{z}_c/(b/2)=-0.172$.

Fig. 3 indicates the layout of aircraft wing--canard wing. The figure shows the distribution of twist angles for different vertical separate positions of aircraft wings and canard wings for the case of $M_\infty=0.85$, $C_{L.D}=0.2$, $a_c=a_w=0.3$, and $\Delta\bar{x}/(b/2)=0.077$.

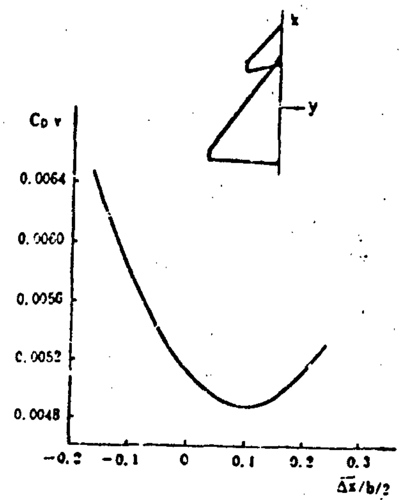

$a_c=a_w=0.3$, $C_{L.D}=0.2$, $M_\infty=0.85$, $\bar{z}_c/(b/2)=-0.172$,

Fig. 1. Distribution of Induced Drag for Configuration of Aircraft Wing--Canard Wing

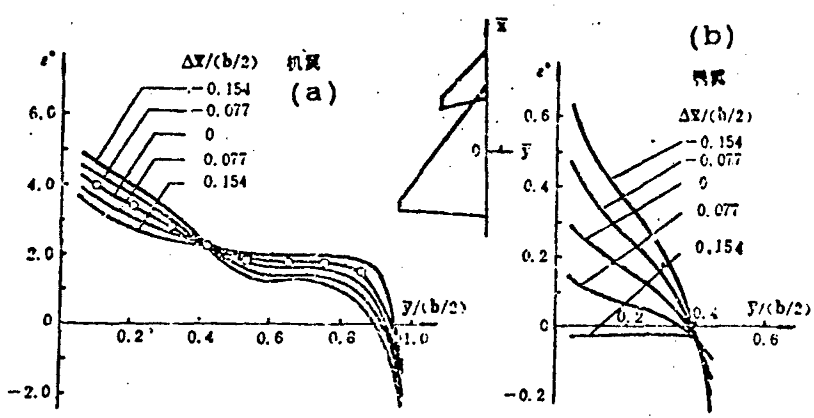

Fig. 2. Distribution of Twist Angles for Configuration of Aircraft Wing--Canard Wing Within the Range of Distributed Flat Points or Force Moment. $\bar{z}_c/(b/2)=-0.172$, $M_\infty=0.85$, $a_c=a_w=0.3$, $C_{L,D}=0.2$
KEY: (a) Canard wing (b) Aircraft wing

Altogether, 15 examples were computed by using the program presented in this paper, which presents the computational results for one example out of the 15.

Fig. 4 presents a layout of canard wing--aircraft wing, showing the distribution of pressure differences prior to and after bending-twisting of four profiles at inner and outer side of the aircraft wing when $M_\infty = 1.5$ and $a=4^o$. In the profile near the wing root prior to bending-twisting, the pressure difference at the leading edge is considerably reduced under the action of the downstream flow field of the canard wing. As indicated by the pressure difference after bending-twisting, the pressure difference at the leading edge increases considerably; the pressure difference is lowered somewhat at the trailing edge. Thus, the pressure difference becomes moderate along the chord direction.

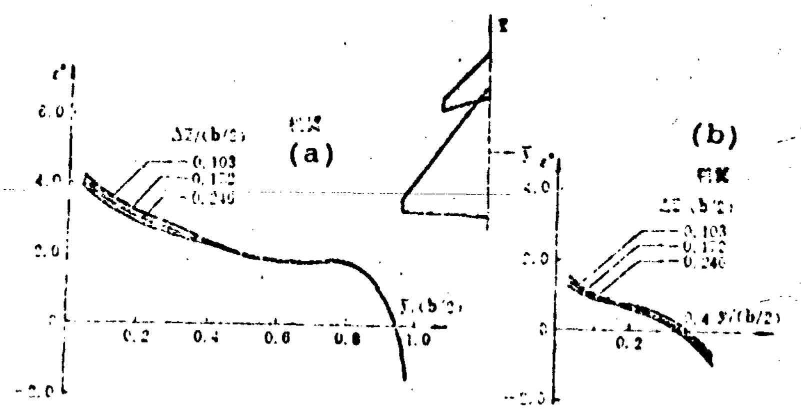

$\Delta \bar{\chi}/(b/2) = 0.077,\ M_\infty = 0.85,\ C_{L,D} = 0.2$

Fig. 3. Distribution of Twist angles for Layout of Aircraft Wing--Canard Wing for Different Vertical Separate Positions

KEY: (a) Aircraft wing (b) Canard wing

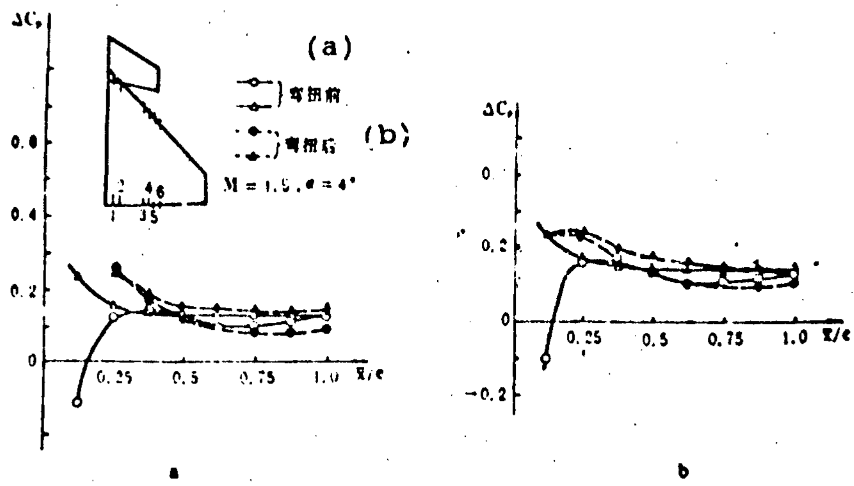

Fig. 4. Distribution of Pressure Difference Between Profiles Near the Inner Side of Root (and Outer Side) of Rear Wing
KEY; (a) Prior to bending-twisting
(b) After bending-twisting

Fig. 5 shows the exterior diagram of canard wing--aircraft wing as well as the shape of bent curved surface thus designed. Under the action of the canard wing (the canard wing is mounted higher than the aircraft wing), this is bending upward from trailing to the leading edge at the wing root profile root; it is bending downward for the wing tip profile; and it is locally transitional at mid-profile. In the situation of limited lift and force moment, the lift-induced drag is reduced from 0.0133 to 0.011z.

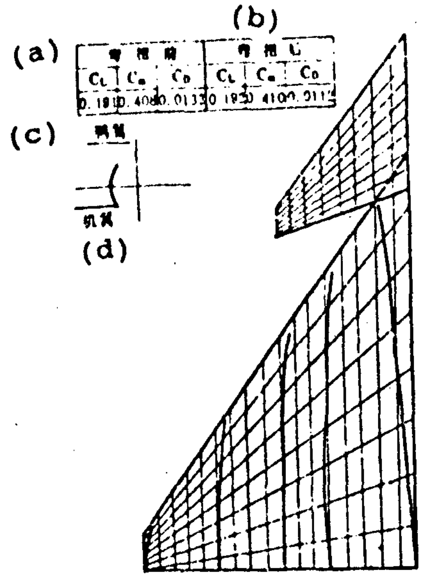

Fig. 5. Shape of Bending-Twisting at Exterior of Noncoplanar Canard Wing--Aircraft Wing Assembly, and Wing Surface: $M_\infty=1.5$, $\alpha=4°$

KEY; (a) Prior to bending-twisting
(b) After bending-twisting
(c) Canard wing
(d) Aircraft wing

Comprehensive bending-twisting design for subsonic aircraft wing

The paper presents the design computational result of the configuration of canard wing--aircraft wing with flap at leading edge. The design state is as follows: at subsonic velocities, M =0.85 and $C_{L.D}$=0.2; at supersonic velocities, M =1.4 and $C_{L.D}$=0.2.

Fig. 6 presents the distribution of bending in an aircraft wing; the figure indicates the gradual increase in bending in the aircraft wing from wing root to wing tip. As a result of supersonic air velocity, an inflexion appears between y/(b/2) =

0.3 and 0.45.

Fig. 7 presents the distribution of twist angle at the aircraft wing during bending-twisting design and comprehensive design at subsonic and supersonic air velocities.

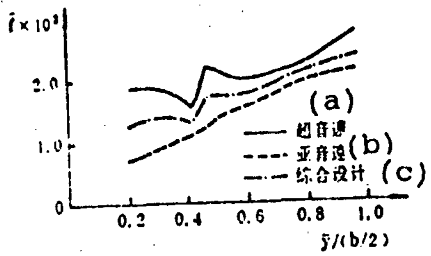

Fig. 6. Camber Distribution at Aircraft Wing With the Optimal Bending-Twisting Design and Comprehensive Design

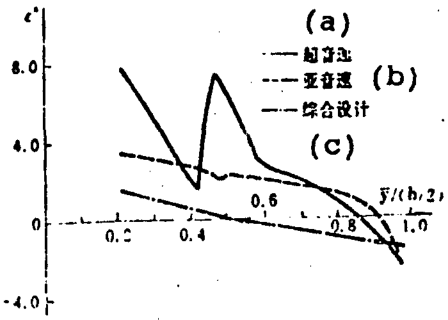

Fig. 7. Twist-Angle Distribution at Aircraft Wing With Optimal Bending-Twisting Design and Comprehensive Design

KEY (for Figs. 6 and 7): (a) Supersonic velocity (b) Subsonic velocity (c) Comprehensive design

Fig. 8 presents polar curves for induced drag with three variants of optimal design, comprehensive design and deviating flap at subsonic air velocities. From the figure, the factor of induced drag increases apparently after the comprehensive tradeoff design: from 0.1410 to 0.1670. By appropriately selecting deviation of the leading-edge flap locally, drag can be reduced.

Fig. 9 presents polar curves for the lift-induced drag at three variants of optimal design, comprehensive design and deviating flap at supersonic air velocities. A similar trend is exhibited in Figs. 8 and 9. The lift-induced drag can be reduced by deviating the flap.

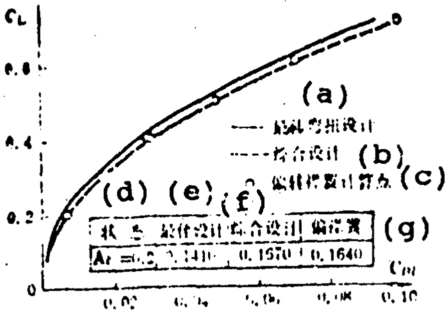

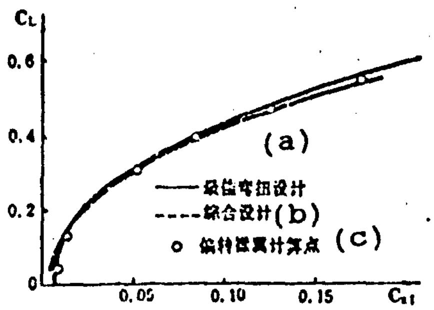

Fig. 8. Polar Curves for Induced Drag With Three Variants at Subsonic Air Velocities

Fig. 9. Polar Curves for Lift-Induced Drag With Three Variants at Supersonic Air Velocities

KEY (for Figs. 8 and 9): (a) Optimal bending-twisting design (b) Comprehensive design (c) Calculation point of deviating flap (d) State (e) Optimal design (f) Comprehensive design (g) deviating flap

As shown in the above-mentioned results, the results of the design computations are rational. The program can be used in first-stage design of bending-twisting aircraft wings.

IV. Conclusions

This paper systematically presents a computational method in the optimal bending-twisting comprehensive design for subsonic and supersonic aircraft wings. Features of this method simultaneously make allowance for the aerodynamic performance aspects at two design points for subsonic and supersonic aircraft, and also consider the requirements imposed by other aircraft performance aspects and structures, thus obtaining the rational bending-twisting shape of the aircraft wing. As explained by analyzing the computational examples, rational results can be obtained with calculations that rely on computer program of such a comprehensive design.

First draft of the paper was received on 8 August 1987. The revised, final draft was received on 17 March 1988.

REFERENCES

[1] Margason, R. J. and Lamar, J. E., NASA TND-6142.
[2] Lamar, J. E., NASA TND-8090.
[3] Woodward, F. A., NASA CR-69181.

[4] Zhu, Guolin et al, Preliminary Conclusion on Applying the Fundamental Solution of Supersonic Air Velocity, Institute No. 1702, 1977.

[5] Li Yupu, Explanation on Overall Control Program on the Optimal Bending-Twisting Comprehensive Design of Aircraft Wing, Institute No. 611, Ministry of Aeronautics and Astronautics Industry, 1986.

DISTRIBUTION LIST

DISTRIBUTION DIRECT TO RECIPIENT

ORGANIZATION	MICROFICHE
B085 DIA/RTS-2FI	1
C509 BALLOC509 BALLISTIC RES LAB	1
C510 R&T LABS/AVEADCOM	1
C513 ARRADCOM	1
C535 AVRADCOM/TSARCOM	1
C539 TRASANA	1
Q592 FSTC	4
Q619 MSIC REDSTONE	1
Q008 NTIC	1
Q043 AFMIC-IS	1
E051 HQ USAF/INET	1
E404 AEDC/DOF	1
E408 AFWL	1
E410 ASDTC/IN	1
E411 ASD/FTD/TTIA	1
E429 SD/IND	1
P005 DOE/ISA/DDI	1
P050 CIA/OCR/ADD/SD	2
1051 AFIT/LDE	1
P090 NSA/CDB	1
2206 FSL	1

Microfiche Nbr: FTD93C000173L
FTD-ID(RS)T-0826-92

END

FILMED

DATE: 4-93

DTIC